Toward Multidimensional Assignment Data Association in Robot Localization and Mapping

W. Sardha Wijesoma, *Member, IEEE*, L. D. L. Perera, and Martin D. Adams

***Abstract*—It is well accepted that the data association or the correspondence problem is one of the toughest problems faced by any state estimation algorithm. Particularly in robotics, it is not very well addressed. This paper introduces a multidimensional assignment (MDA)-based data association algorithm for the simultaneous localization and map building (SLAM) problem in mobile robot navigation. The data association problem is cast in a general discrete optimization framework and the MDA formulation for multitarget tracking is extended for SLAM using sensor location uncertainty with the joint likelihood of measurements over multiple frames as the objective function. Methods for feature initialization and management are also integrated into the algorithm. When clutter is high and features are sparse, the compatibility information of features of a single measurement frame is not sufficient to make effective data-association decisions, thus compromising performance of single-frame-based methods. However, in a multiple-measurement-frame approach, the availability of more than one frame of measurement provides for more effective data-association decisions to be made, as consistency of measurements are looked at in several frames of measurement. Simulations are conducted to verify the performance gains over the conventional nearest neighbor (NN) data association algorithm and the joint compatibility branch and bound (JCBB) algorithm, especially in the presence of varying densities of spurious measurements and dynamic objects. Experimental results with ground truth are presented to demonstrate the practicality of the proposed data-association method in complex and large outdoor environments and its effectiveness over single-frame-based NN and JCBB schemes.**

***Index Terms*—Data association, localization, robot navigation, tracking.**

NOMENCLATURE

N	Number of frames.
k	Current time.
$\mathbf{Z}(k)$	Set of measurements obtained in frame k.
$\mathbf{z}_{i(l)}$	ith measurement obtained in frame l.
$n(l)$	Number of actual measurements obtained in frame l.
Ω	Partition of assigning features to measurements.
T	Number of features in the state vector.
Ξ	Data-association cost function.
$\Lambda(\Omega)$	Likelihood function of the partition Ω.
Λ_{true}	Likelihood of assigning true features.
Λ_{false}	Likelihood of measurements associating with spurious measurements (or clutter).
V_S	Operating region.
$T(l)$	Detected features in frame l.
Γ	Set of all features.
$\boldsymbol{\tau}_t$	A feature in Γ.
$\varepsilon(i(l))$	A variable specifying 1 if $i(l) \neq 0$ or 0 if $i(l) = 0$.
$\eta(t, i(k-N+1), \ldots, i(k))$	Association variable specifying the measurement sequence $\mathbf{z}_{i(k-N+1)}$, $\mathbf{z}_{i(k-N+2)}, \ldots, \mathbf{z}_{i(k)}$ is associated with feature $\boldsymbol{\tau}_t$.
$c(t, i(k-N+1), \ldots, i(k))$	Cost of associating measurement sequence $\mathbf{z}_{i(k-N+1)}$, $\mathbf{z}_{i(k-N+2)}, \ldots, \mathbf{z}_{i(k)}$ with feature $\boldsymbol{\tau}_t$.

I. INTRODUCTION

THE simultaneous localization and mapping (SLAM) problem, also known as concurrent mapping and localization (CML) problem, is often recognized in the robotics literature as one of the key challenges in building autonomous capabilities for mobile vehicles. The goal of an autonomous vehicle performing SLAM is to start from an unknown location in an unknown environment and build a map (consisting of environmental features) of its environment incrementally by using the uncertain information extracted from its sensors, whilst simultaneously using that map to localize itself with respect to a reference coordinate frame and navigate in real time.

A vehicle capable of performing SLAM using naturally occurring environmental features and capable of running for hours or possibly days in completely unknown and unstructured environments will indeed be invaluable in several key areas of robotics. These include autonomous vehicle operation in

Manuscript received November 30, 2004; revised June 27, 2005. This paper was recommended for publication by Associate Editor K. Yoshida and Editor S. Hutchinson upon evaluation of the reviewers' comments. This paper was presented in part at the IEEE International Conference on Robotics and AutomationNew Orleans, LA, April 26–May 1, 2004.

The authors are with the Division of Control and Instrumentation, School of Electrical and Electronic Engineering, Nanyang Technological University, Singapore 639798 (e-mail: eswwijesoma@ntu.edu.sg).

Digital Object Identifier 10.1109/TRO.2006.870634

unstructured terrain, driver-assistance systems, mining, surveying, cargo handling, autonomous underwater explorations, aviation applications, autonomous planetary exploration, and military applications. The first solution to the SLAM problem was proposed by Smith *et al.* [1]. They emphasized the importance of map and vehicle correlations in SLAM and introduced the extended Kalman filter (EKF)-based stochastic mapping framework, which estimated the vehicle pose and the map feature (landmark) positions in an augmented state vector using second order statistics. Although EKF-based SLAM within the stochastic mapping framework gained wide popularity among the SLAM research community, over time, it was shown to have several shortcomings [2], [3]. Notable shortcomings are its susceptibility to data-association errors and inconsistent treatment of nonlinearities.

Data association, registration, or the correspondence problem is one of the extremely difficult problems encountered in SLAM even in static environments and much more challenging in dynamic environments consisting of objects moving at varying velocities. Almost every state estimation algorithm has to deal with the correspondence problem in the form of maximum-likelihood assignment or correlation search in establishing the correspondence between the elements of observations and the available features. Uncertainties in vehicle pose, variable feature densities, dynamic objects in the environment, and spurious measurements complicate data association in the SLAM problem in many respects. An efficient data-association scheme must aid feature or track initialization, maintenance, termination, and map management.

It is established that the feature-based approach to SLAM can be considered as a multisensor multitarget tracking problem [2]. This method is highly sensitive to the fragility of data association (incorrect measurement to feature associations). Misassociations invariably result in map inconsistency and divergence. An efficient and effective data-association scheme must establish the difference amongst spurious measurements, new measurements, and missed detections in addition to the basic function of associating currently available features with measurements. The most widely employed data-association method in SLAM is the nearest neighbor (NN) data-association algorithm [3], [13]. It associates a feature to the nearest observation in a chosen validation region based on some distance measure, which is usually the Mahalanobias distance. Although it is quite easy to implement, in moderate and high clutter (spurious measurements), its performance is poor. Further, data-association decisions are hard, meaning that decisions once made cannot be reversed. Joint probabilistic data association (JPDA) [4], [14], [15] emerged to provide a better solution to the clutter or spurious measurements and ambiguities of the NN method. JPDA associates all of the measurements falling inside a suitably chosen validation region of a track to itself by a probabilistic weighting procedure and performs relatively well when spurious measurements are relatively moderate. The downside is that it can be computationally prohibitive in terms of calculating weighting probabilities, and the process may corrupt the feature recognition or discrimination information. Further, JPDA is a single-frame hard-decision approach and, in its standard form [4], does not explicitly provide a means of initiating tracks, which is vital for feature-based map-building applications. The joint compatibility branch and bound (JCBB) method, which takes groups of feature- (track-) observation associations into consideration in the context of searching for the hypothesis with the maximum number of compatible pairs, is also well known for its effectiveness in SLAM [23] for data association. Compared with other methods, JCBB takes into account the full spatial correlations between vehicle and features in making data-association decisions. However, the resultant exponential search space, despite the branch and bound pruning, renders the technique computationally intensive for real-time implementation in moderate-sized outdoor environments with a large number of spurious measurements and dynamic objects. JCBB also makes hard decisions, which cannot be reversed over time and, further, only takes into account the measurements in the current time frame and ignores temporal attributes of the collective measurements in its decision making.

Multiple hypotheses tracking (MHT) [5], [14], [16] is the most structured and optimal approach employing deferred logic available for multitarget tracking and data association. Deferred logic schemes allow data-association decisions to be delayed until a number of additional frames of measurements are received in successive scans so that incorrect associations made in the past can be corrected if necessary. For example, MHT defers the association decisions in conflicting situations and forms a tree of all probable association hypotheses, which are then propagated through subsequent iterations in the belief that new information will most likely resolve conflicts, if any. Therefore, MHT is capable of dealing with missed detections, spurious measurements, and track initiation. However, the major drawback of MHT is that the hypothesis tree grows exponentially in time, requiring exponential memory and computational resources, making it impracticable and unsuitable for real-time implementation. A variant of MHT known as the "lazy" data-association method [24] picks the most likely data association when a feature is observed as in a maximum-likelihood data association (MLDA) method [3]. However, unlike in MLDA, it stores and monitors the past and current data to detect whether different data associations (traversals of the hypothesis tree) can yield a map and path posterior of higher likelihood and, hence, revise the past data-association decisions. However, use of all past correspondence variables in the method still makes it exponentially complex, requiring heuristics and other *ad-hoc* strategies to prune the search space for real-time implementation. In [25], Nieto *et al.* proposes an MHT method for FastSLAM [11]. This method splits each particle representing a map in FastSLAM into further particles for keeping association hypotheses. The particles with wrong data associations are expected to die out in the resampling stage. The main disadvantage of this method is that the number of particles required for implementation of the algorithm can increase without bound, thus causing computational problems.

The MDA method used in this study, on the other hand, has received extensive attention in aircraft tracking and is believed to find widespread use in most future multitarget tracking and surveillance systems [14], even going to the extent of replacing the optimal but computationally infeasible MHT. This paper

proposes, and makes use of, the MDA algorithm for the first time into the much harder tracking and data-association problems encountered in robot localization and map building, where sensor location uncertainty has to be incorporated. The use of this method is largely justified on the basis that single-frame data-association methods frequently fail in SLAM when features are not sparsely distributed or in the presence of high, temporally persistent clutter or dynamic objects. Further, multiple-frame-based methods are more computationally intensive. MDA methods in multitarget tracking and data association have comparable performance with MHT and lower computational complexity than MHT and JPDA and therefore are a viable option for the real-time data-association requirements of robot navigation applications.

This paper is organized in the following manner. Section II briefly reviews previous work on MDA-based data-association approaches and introduces the general framework for multiple-frame data association. Integer-programming (IP) formulation of the MDA data association is then presented. Section III describes in detail the formulation and application of MDA with two frames of measurements for EKF-based SLAM. Section IV describes the performance of MDA in SLAM and how it compares with the common and efficient NN data-association algorithm and the very effective, although computationally intensive, data-association JCBB algorithm. Experimental results are then presented to demonstrate the efficiency of the algorithm in real large, moderate, and small-sized outdoor environments. Section V discusses the merits and demerits of the proposed methodology, and Section VI concludes the paper with possible ways it could be further extended.

II. Data Association as a Multiple-Frame Multidimensional Assignment Problem

A. General Multidimensional Assignment Data Association

MHT generates a set of hypotheses over several frames of measurements and uses a special form of MDA methodology in selecting the most appropriate hypothesis of track to measurement associations. However, exponential computational requirements, even under aggressive pruning strategies, limit the application of MHT in real-time multitarget tracking systems. An alternative to this is proposed in [6], in which multiple-frame data association in the context of multitarget tracking is formulated as a discrete optimization problem. This is further extended in [7]–[9] by expressing data association of multiple targets over multiple frames, in the form of an MDA problem. The core attribute of these algorithms can be identified as the use of more than one frame of measurement in determining the best associations for the current frame. In this study, the data-association problem is formulated as a generic MDA problem and is applied in the context of real-time robot concurrent localization and mapping.

B. Data Association as a Generalized Discrete Optimization Problem

In this section, the notation and formulation of the generalized N-frame multidimensional data association, as an optimization problem, is given. A summary of the notation is also included at the beginning of the paper in the Nomenclature for easy reference. Suppose that, over the period of time $[k-N+1,k]$, N frames of measurement are obtained at time instances, $k-N+1, k-N+2, \ldots, k-1$, and k. Let the set of map features available and updated at time $k-N$ be $\mathbf{\Gamma} = \{\boldsymbol{\tau}_t | t = 1, 2, \ldots\ldots\ldots, T\}$. Now, the problem of multidimensional-assignment data association is to assign proper measurement combinations of the N frames of measurement to the T features in an optimal and efficient manner subject to certain constraints.

Let the set of measurements obtained in a frame l be $\mathbf{Z}(l) = \{\mathbf{z}_{i(l)} | i(l) = 0, 1, 2, \ldots\ldots\ldots, n(l)\}$, where $n(l)$ is the actual number of measurements and $i(l) = 0$ corresponds to a dummy or fictitious measurement used to accommodate any missed detections of features. Let Ω denote a specific but complete assignment of the T features to the measurements in the N consecutive measurement frames. In other words, Ω is a partition of the product space $\Theta = \mathbf{Z}(k-N+1) \times \mathbf{Z}(k-N-2) \times \ldots\ldots \times \mathbf{Z}(k) \times \Gamma$ of measurements in N frames and T features in Γ. Now, the solution to the multiple-frame data-association problem can be formulated in general as a discrete optimization problem minimizing some appropriately chosen cost function $\Xi(\Omega)$, relating the measurements in N frames to T features subject to a set of constraints.

For example, if the cost function $\Xi(\Omega)$ used in this general framework is the sum of distances between the T features and measurements in each frame, the result is a nonlinear optimization problem resembling N-frame NN data association. When $N = 1$, we have the standard NN data-association algorithm.

Although one could use many criteria, a cost function based on the joint likelihood between features and measurements in multiple frames is used so that the resulting solution is optimal in the sense of maximum likelihood over multiple frames. In multiple-target tracking from a stationary sensor, when targets move independently, the joint likelihood of measurements in a frame can be determined by the product of the likelihoods of the absolute measurements, as these are not correlated. However, in SLAM, the sensors are on board the moving vehicle and, as such, the location uncertainty of the sensors (vehicle) needs to be taken in to account. Furthermore, the measurements and features are correlated over the vehicle state. Thus, these feature measurements depend on the common underlying vehicle state at a given instant. In general, it is reasonable to assume that the underlying vehicle state is the only thing in common between the measurements' sources. Therefore, once the state of the vehicle and the feature map has been specified, it is reasonable to assume that the measurements in a frame are conditionally independent. As such, and for reasons of simplicity and mathematical tractability, conditional measurement independence is assumed as in [3] [15] to derive the joint-likelihood function $\Lambda(\Omega)$ involving the N measurement frames and the T features for a partition Ω of Θ in a manner similar to [7]. However, the joint likelihoods are calculated using relative feature measurements, incorporating sensor location uncertainty. The joint likelihood can be expressed as

$$\Lambda(\Omega) = \Lambda_{\text{true}}(\Omega)\Lambda_{\text{false}}(\Omega) \tag{1}$$

where $\Lambda_{\text{true}}(\Omega)$ and $\Lambda_{\text{false}}(\Omega)$ are the joint likelihoods of measurements associating with true features and spurious measurements, respectively, in the partition Ω.

Now, if the spurious measurements (or in general clutter) are uniformly distributed in the operating region V_S, then $\Lambda_{\text{false}}(\Omega)$ can be obtained as follows:

$$\Lambda_{\text{false}} = \prod_{l=k}^{l=k-N+1} \left(\frac{1}{V_s}\right)^{n(l)-T(l)} \tag{2}$$

where $T(l)$ is the number of feature detections in the frame l. Given a feature $\boldsymbol{\tau}_t$, the likelihood of the ith measurement $\mathbf{z}_{i(k-N+1)}$ in frame $k-N+1$ (first frame in the sequence of N frames) is represented as $L(\mathbf{z}_{i(k-N+1)}|\boldsymbol{\tau}_t)$. Then, the likelihood of the ith measurement $\mathbf{z}_{i(k-N+2)}$, in frame $k-N+2$ given feature $\boldsymbol{\tau}_t$ and a measurement $\mathbf{z}_{i(k-N+1)}$ in frame $k-N+1$, is $L(\mathbf{z}_{i(k-N+2)}|\mathbf{z}_{i(k-N+1)}, \boldsymbol{\tau}_t)$. In a similar manner, we could express the likelihood of the ith measurement $\mathbf{z}_{i(k-m)}$ in a frame $k-m$ given the feature $\boldsymbol{\tau}_t$ and the measurements $\mathbf{z}_{i(k-N+1)}, \mathbf{z}_{i(k-N+2)}, \cdots, \mathbf{z}_{i(k-m+1)}$ from frame $k-N+1$ leading up to the frame $k-m$ as $L(\mathbf{z}_{i(k-m)}|\mathbf{z}_{i(k-N+1)}, \ldots, \mathbf{z}_{i(k-m-1)}, \boldsymbol{\tau}_t)$. Now, if the detection probability of a feature is assumed constant and equal to p_d, then it can be verified that the joint likelihood Λ_{true} of measurements associating with T features for the partition Ω is

$$\begin{aligned}\Lambda_{\text{true}}(\Omega) = &\prod_{\forall t} \left(p_d L\left(\mathbf{z}_{i(k-N+1)}|\boldsymbol{\tau}_t\right)\right)^{\varepsilon(i(k-N+1))} \\ &\times (1-p_d)^{1-\varepsilon(i(k-N+1))} \\ &\times \left(p_d L\left(\mathbf{z}_{i(k-N+2)}|\mathbf{z}_{i(k-N+1)}, \boldsymbol{\tau}_t\right)\right)^{\varepsilon(i(k-N+2))} \\ &\times (1-p_d)^{1-\varepsilon(i(k-N+2))} \cdots\cdots\cdots \\ &\left(p_d L\left(\mathbf{z}_{i(k)}|\mathbf{z}_{i(k-N+1)}, \ldots, \mathbf{z}_{i(k-1)}, \boldsymbol{\tau}_t\right)\right)^{\varepsilon(i(k))} \\ &\times (1-p_d)^{1-\varepsilon(i(k))}\end{aligned} \tag{3}$$

where

$$\varepsilon(i(l)) = \begin{cases} 1, i(l) \neq 0 \\ 0\, i(l) = 0 \end{cases} \quad l = k, \ldots, (k-N+1)$$

i.e., $\varepsilon(i(l))$ is 0 when associating feature $\boldsymbol{\tau}_t$ to the dummy measurement $(i(l)=0)$ in frame l and 1 when it is associated with a true measurement. The joint likelihood $\Lambda(\Omega)$ is obtained by substituting (3) and (2) into (1). A normalized joint likelihood denoted by $\Lambda_N(\Omega)$ can now be arrived at as

$$\Lambda_N(\Omega) = \frac{\Lambda(\Omega)}{\left(V_s^{-n(k)} V_s^{-n(k-1)} \ldots\ldots V_s^{-n(k-N+1)}\right)}. \tag{4}$$

Now, the data-association problem can be expressed as searching for a partition Ω that minimizes the cost function equal to the minus log-likelihood value of $\Lambda_N(\Omega)$

$$\begin{aligned}\Xi(\Omega) &= -\ln\left(\Lambda_N(\Omega)\right) \\ &= \sum_{\Omega} c\left(t, i(k-N+1), \ldots, i(k-1), i(k)\right). \end{aligned} \tag{5}$$

It is easy to see that searching for Ω that minimizes $\Xi(\Omega)$ is equivalent to the assignment of one measurement from each of the N frames, to each feature $\boldsymbol{\tau}_t (t = 1, 2, \ldots, T)$ with an associated cost of $c(t, i(k-N+1), \ldots, i(k-1), i(k))$ (which can be deduced from (3) and specified here as c for clarity) subject to an appropriate set of constraints. The problem is one of multidimensional assignment. The search for the optimal association over multiple frames can be accomplished as follows.

Let an association variable $\eta(t, i(k-N+1), \ldots, i(k-1), i(k))$ (specified as η here onwards for clarity) be defined in such a way that $\eta = 1$ when a sequence of measurements $\mathbf{z}_{i(k-N+1)}, \mathbf{z}_{i(k-N+2)}, \ldots, \mathbf{z}_{i(k)}$ from the N successive frames are associated with the feature $\boldsymbol{\tau}_t$, and $\eta = 0$, otherwise. The search for Ω that minimizes $\Xi(\Omega)$ can therefore be obtained by solving the following nonlinear 0–1 integer programming problem:

$$\text{Minimize} \sum_{i(k-N+1)=0}^{n(k-N+1)} \cdots \sum_{i(l)=0}^{n(l)} \cdots\cdots\cdots \sum_{i(k)=0}^{n(k)} \sum_{t=1}^{T} \eta c \tag{6}$$

subject to the following constraints imposed on the association variables.

1) Each measurement, except for dummy measurements, can be assigned to only one or no features in the map. However, the dummy measurement $(i(l)=0)$ in a frame l can be assigned to more than one feature, as there can be several undetected features in a scan. Thus, we have the single source constraint for measurements

$$\sum_{i(k-N+2)=0}^{n(k-N+2)} \cdots\cdots \sum_{i(k)=0}^{n(k)} \sum_{t=1}^{T} \eta \leq 1, \quad i(k-N+1) = 1, 2, \ldots, n(k-N+1) \tag{7}$$

$$\sum_{i(k-N+1)=0}^{n(k-N+1)} \cdots\cdots \sum_{i(k-1)=0}^{n(k-1)} \sum_{t=1}^{T} \eta \leq 1, \quad i(k) = 1, 2, \ldots, n(k) \tag{8}$$

$$\sum_{i(k-N+1)=0}^{n(k-N+1)} \cdots\cdots \sum_{i(k-m-1)=0}^{n(k-m-1)} \sum_{i(k-m+1)=0}^{n(k-m+1)} \cdots\cdots \sum_{i(k)=0}^{n(k)} \sum_{t=1}^{T} \eta \leq 1 \quad \forall i(k-m) = 1, 2, \ldots, n(k-m), \; m = N-2, N-3, \ldots, 1. \tag{9}$$

2) Each feature $\boldsymbol{\tau}_t$ can generate only one measurement in one measurement frame, which gives the single return constraint

$$\sum_{i(k-N+1)=0}^{n(k-N+1)} \cdots\cdots \sum_{i(k)=0}^{n(k)} \eta = 1, \quad t = 1, 2, \ldots, T. \tag{10}$$

Constraint (10) therefore consists of T constraint equations.

3) The maximum missed detections of features in a measurement frame cannot exceed the number of existing features in the map. Therefore, the possibility of obtaining a missed detection for each feature in every measurement frame is

considered. Thus, the constraints on the maximum number of dummy measurements are

$$\sum_{i(k-N+2)=0}^{n(k-N+2)} \cdots \sum_{i(k)=0}^{n(k)} \sum_{t=1}^{T} \eta\left(t, 0, \ldots, i(k-1), i(k)\right) \leq T \quad (11)$$

$$\sum_{i(k-N+1)=0}^{n(k-N+1)} \cdots \sum_{i(k-m-1)=0}^{n(k-m-1)} \sum_{i(k-m+1)=0}^{n(k-m+1)} \cdots \sum_{i(k)=0}^{n(k)} \sum_{t=1}^{T} \eta_m \leq T, \quad m = N-2, \ldots, 1 \quad (12)$$

where $\eta_m = \eta$ with $i(k-m) = 0$

$$\sum_{i(k-N+1)=0}^{n(k-N+1)} \cdots \sum_{i(k-1)=0}^{n(k-1)} \sum_{t=1}^{T} \times \eta\left(t, i(k-N+1), \ldots, i(k-1), 0\right) \leq T. \quad (13)$$

4) By definition, the association variable η must be either 0 or 1. Thus, the following 0–1 integer constraints apply:

$$\eta = \{0,1\} \quad \forall i(k-N+1), \ldots, i(k-1), i(k), \ t = 1, 2, \ldots, T. \quad (14)$$

The 0–1 integer-programming problem (1)–(14) is NP hard. To simplify its application to SLAM, a suboptimal solution can be obtained by relaxing the 0–1 integer constraint (14) on η to a nonnegativity constraint as follows:

$$\eta \geq 0 \quad \forall i(k-N+1), \ldots, i(k), \quad t = 1, 2, \ldots, T. \quad (15)$$

MDA for the specific case of two frames is given in Appendix II to aid understanding of the generalized N-frame formulation given above.

III. Data Association in Feature-Based SLAM

To keep the computational complexity manageable, the application of the MDA method for data association in SLAM is rigorously formulated and illustrated for two consecutive frames of measurements. The use of more than two measurement frames can be accommodated easily using the generalized formulation in Section II. Limiting the measurement frames to two reduces the problem to a three-dimensional (3-D) assignment problem. The resulting 0–1 integer (nonlinear) program is then adapted to a linear programming problem, for a polynomial time suboptimal solution. This linear programming problem is then solved by Mehrotra's predictor corrector method [12], which is a primal-dual interior-point method. This algorithm is a faster version of the kind of interior point algorithms available for solving large scale linear programming problems known as primal-dual infeasible interior point methods. Unlike primal methods, which concentrate on solving the primal problem, primal-dual interior-point methods solve the Karush–Kuhn–Tucker (KKT) system of a linear program, which includes primal, dual, and slack variables. These methods solve the KKT system of equations using a damped Newton's method with a step size determined to satisfy all of the nonnegativity constraints. Mehrotra's method has a worst case arithmetic complexity of $O(n^3)$ and $O(nL)$ iteration complexity [12], where n is the dimension of the data set and L is the bit length of data that relates to the number of association hypotheses.

A. Review of Feature-Based SLAM

For simplicity, an EKF-based stochastic mapping approach is employed in this formulation, although it can be easily extended to cater to the Rao–Blackwellised particle filter-based methods [10], [11] and numerous other methods of SLAM formulations [17]–[19]. The methodology is still considered to be the primary framework of most feature-based stochastic SLAM algorithms [1], [3] and is also used in this study to illustrate multidimensional data association for SLAM. The major highlight of the formulation is its consistent probabilistic representation of the pose of the vehicle (or robot), the positions of features, their uncertainties, and their interrelationships. In the EKF-SLAM formulation, the pose of the vehicle and the positions of features are concatenated to form an augmented or composite state vector $\mathbf{X}(k)$. The pose of vehicle (robot) $\mathbf{x}_v(k)$ and feature locations $\mathbf{m}(k)$ (known as the map) at a time instant k are represented by absolute coordinates with reference to a global coordinate frame. In the following, the EKF-based SLAM solution is stated for a vehicle traversing a 2-D terrain with point features or landmarks in the environment. The vehicle-map composite or SLAM state vector $\mathbf{X}(k)$ at time instant k is thus

$$\mathbf{X}(k) = \begin{bmatrix} \mathbf{x}_v^T(k) & \mathbf{m}^T(k) \end{bmatrix}^T \quad (16)$$

where $\mathbf{x}_v(k) = [x(k)\ y(k)\ \theta(k)]^T$ is the vehicle pose with $x(k)$, $y(k)$, and $\theta(k)$ denoting position coordinates and heading of the vehicle and $\mathbf{m}(k) = [x_1(k)\ y_1(k)\ \ldots\ldots\ x_n(k)\ y_n(k)]^T$ is the vector of feature positions with $[x_i(k)\ y_i(k)]^T$, $i = 1, 2, \ldots, n$ denoting the feature coordinates with respect to the global coordinate frame. In general, the motion model of the vehicle is nonlinear and can be represented in closed form as

$$\mathbf{x}_v(k) = \mathbf{f}\left(\mathbf{x}_v(k-1), \mathbf{u}(k-1)\right) + \mathbf{n}(k) \quad (17)$$

where $\mathbf{u}(k-1)$ is the control input at time $k-1$ and $\mathbf{n}(k)$ is a zero-mean temporally uncorrelated noise sequence with covariance matrix $\mathbf{Q}_v(k)$. Assuming static features (landmarks), the process model of the feature map is

$$\mathbf{m}(k) = \mathbf{m}(k-1). \quad (18)$$

The observation model is represented by

$$\mathbf{z}(k) = \mathbf{h}\left(\mathbf{x}_v(k), \mathbf{m}(k)\right) + \mathbf{w}(k) \quad (19)$$

where $\mathbf{w}(k)$ is a zero-mean temporally uncorrelated noise sequence with covariance matrix $\mathbf{R}(k)$. When the covariance matrix of the composite state vector $\mathbf{X}(k)$, which is known as the

composite covariance matrix, is denoted by $\mathbf{P}(k)$, and the observation prediction is specified by $\widehat{\mathbf{z}}(k)$, then the EKF predictor equations are as follows:

$$\mathbf{X}(k|k-1) = \left[\left(\mathbf{f}\left(\mathbf{x}_v(k-1), \mathbf{u}(k-1)\right)\right)^T \quad \mathbf{m}^T(k-1)\right]^T \tag{20}$$

$$\mathbf{P}(k|k-1) = \mathbf{F}\mathbf{P}(k-1|k-1)\mathbf{F}^T + \mathbf{Q}(k) \tag{21}$$

$$\widehat{\mathbf{z}}(k) = \mathbf{h}\left(\mathbf{x}_v(k|k-1), \mathbf{m}(k|k-1)\right) \tag{22}$$

where $\mathbf{F}$ is the Jacobian $(\partial \mathbf{X}(k|K-1)/\partial \mathbf{X})$ of the composite process model (20) evaluated at time $k-1$ and $\mathbf{Q}(k)$ is the composite process noise covariance matrix. When observations $\mathbf{z}(k)$ are made at time k, and after correct observation to feature associations are resolved using an appropriate data association algorithm, then the EKF update equations are applied as follows:

$$\mathbf{v}(k) = \mathbf{z}(k) - \widehat{\mathbf{z}}(k) \tag{23}$$

$$\mathbf{X}(k|k) = \mathbf{X}(k|k-1) + \mathbf{K}(k)\mathbf{v}(k) \tag{24}$$

$$\mathbf{P}(k|k) = \mathbf{P}(k|k-1) - \mathbf{K}(k)\mathbf{S}(k)\mathbf{K}(k)^T \tag{25}$$

where $\mathbf{v}(k)$ is the observation innovation, $\mathbf{S}(k)$ is its covariance matrix, and $\mathbf{K}(k) = \mathbf{P}(k|k-1)\mathbf{H}^T\mathbf{S}^{-1}(k)$ is the Kalman gain, where $\mathbf{H}$ is the Jacobian $(\partial \mathbf{h}/\partial \mathbf{X})$.

B. Feature Initiation and Map Maintenance

Feature initiation plays a vital role in all SLAM algorithms. When observations are received, they are first associated with the features in the SLAM state vector using the MDA data association. If an association is found, that observation is used to update the composite SLAM state vector. If an association is not found, the observation is considered to be a potential new feature, i.e., a tentative feature, and is added into the state vector, the rationale being that the multidimensional data-association algorithm can effectively remove t spurious measurements and returns due to dynamic objects more effectively than a single frame of measurement schemes, and hence it is logical to add every new (tentative) feature measurement straightaway in to the SLAM state vector as these have a higher possibility of being genuine features. The new (tentative) feature is appended to the full SLAM state vector and the covariance is updated in the following equations and (28), shown at the bottom of the page:

$$\begin{aligned}\mathbf{g}(.) &= \mathbf{x}_{\text{new}}(k) \\ &= \begin{bmatrix} x(k|k) + r_{\text{new}}\cos\left(\theta_{\text{new}} + \theta(k|k)\right) \\ y(k|k) + r_{\text{new}}\sin\left(\theta_{\text{new}} + \theta(k|k)\right)\end{bmatrix}\end{aligned} \tag{26}$$

$$\mathbf{X}_{\text{aug}}(k) = \begin{bmatrix}\mathbf{X}(k|k) \\ \mathbf{x}_{\text{new}}(k)\end{bmatrix} \tag{27}$$

where the new feature's relative range and bearing measurement $\mathbf{z}$ is $(r_{\text{new}}, \theta_{\text{new}})$, the inverse observation function is $\mathbf{g}(.)$, the new augmented state vector is $\mathbf{X}_{\text{aug}}(k)$, its covariance matrix is $\mathbf{P}_{\text{aug}}(k)$, the vehicle covariance matrix is $\mathbf{P}_{vv}(k|k)$, and the Jacobians of $\mathbf{g}(.)$ with respect to $\mathbf{X}(k)$, $\mathbf{x}_v(k)$, and $\mathbf{z}$ are $\nabla_{\mathbf{X}}\mathbf{g}$, $\nabla_v\mathbf{g}$, and $\nabla_{\mathbf{z}}\mathbf{g}$, respectively.

However, it could be that the new features (tentative) added could be spurious measurements and that their frequency of occurrences is dependent on the number of frames used in data association. Thus, as a part of the feature maintenance strategy, the "quality" of these tentative or newly added features are monitored over a number of consecutive frames of measurement. The quality measure used is the number of successive frames (or scans) over which the newly added feature (tentative feature) is successfully associated with measurements using the multidimensional data-association method. If this predetermined number is exceeded, the tentative feature in the SLAM vector is declared confirmed and is used to update the SLAM state, or else it is deleted from the SLAM state vector. That is, only measurements associated with confirmed map features are used to update the SLAM state vector. Of course, to measure the quality of a feature, other criteria may be chosen as well as for maintenance and deletion, as in [16]. To reduce the association variables and, hence, improve computational speed, observations are preprocessed at every scan prior to the application of N-frame data association. Further, the necessary log-likelihood functions and associated cost functions are also computed as described below.

C. Reduction of Association Variables

The number of variables associated with the linear program can be reduced by data preprocessing and gating of measurements. This step eliminates all of the unlikely associations and thereby improves algorithm efficiency. As absolute feature locations and the measurement predictions are correlated over the vehicle state, we use the relative measurements and their predictions in the sections that follow. Let the absolute coordinate of a feature τ_t in the state vector at time $k-2$ be denoted by $\mathbf{x}_t(k-2) = [x_t(k-2)\, y_t(k-2)]^T$. Assuming a range-bearing measurement system such as SICK LMS 290, its relative measurement prediction in frame $k-1$, $\widehat{z}_{i(k-1),t}$, and its covariance matrix $\mathbf{P}_{i(k-1),t}$ are

$$\begin{aligned}\widehat{\mathbf{z}}_{i(k-1),t} &= \begin{bmatrix}\sqrt{a^2+b^2} \\ \tan^{-1}\left(\frac{b}{a}\right) - \theta(k-1|k-2)\end{bmatrix} \\ &= \mathbf{h}\left(\mathbf{x}_v(k-1|k-2), \mathbf{x}_t(k-1|k-2)\right)\end{aligned} \tag{29}$$

where $a = x_t(k-1|k-2) - x(k-1|k-2)$ and $b = y_t(k-1|k-2) - y(k-1|k-2)$

$$\mathbf{P}_{i(k-1),t} = \mathbf{H}\mathbf{P}(k-1|k-2)\mathbf{H}^T \tag{30}$$

where $\mathbf{H}$ is the Jacobian of $\widehat{z}_{i(k-1),t}$ with respect to the state $\mathbf{X}(k-1)$. Let the ith relative measurement $i(k-1)$ in frame $k-1$

$$\mathbf{P}_{\text{aug}}(k) = \begin{bmatrix}\mathbf{P}(k|k) & \mathbf{P}^T(k|k)\nabla_{\mathbf{X}}\mathbf{g}^T \\ \nabla_{\mathbf{X}}\mathbf{g}\mathbf{P}(k|k) & \nabla_v\mathbf{g}\mathbf{P}_{vv}(k|k)\nabla_v\mathbf{g}^T + \nabla_{\mathbf{z}}\mathbf{g}\mathbf{R}(k)\nabla_{\mathbf{z}}\mathbf{g}^T\end{bmatrix} \tag{28}$$

be denoted by $\mathbf{z}_{i(k-1)}$. Then, the innovation $\mathbf{v}_{i(k-1),t}$ and its covariance $\mathbf{S}_{i(k-1),t}$ are calculated for all of the combinations of observations in frame $k-1$ and all of the features $\boldsymbol{\tau}_t$ as follows:

$$\mathbf{v}_{i(k-1),t} = \mathbf{z}_{i(k-1)} - \widehat{\mathbf{z}}_{i(k-1),t} \tag{31}$$

$$\mathbf{S}_{i(k-1),t} = \mathbf{P}_{i(k-1),t} + \mathbf{R}(k-1). \tag{32}$$

Then, the set of measurements $\mathbf{Z}(k-1)$ in frame $k-1$ satisfying the χ^2 statistical test given below is selected for data association:

$$\mathbf{Z}(k-1) = \Big\{ \mathbf{z}_{i(k-1)} | \mathbf{v}_{i(k-1),t}^T \mathbf{S}_{i(k-1),t}^{-1} \mathbf{v}_{i(k-1),t} \leq g_1 \forall i(k-1), t \Big\} \tag{33}$$

where g_1 is a threshold determined from the χ^2 distribution of $\dim(\mathbf{z}_{i(k-1)})$ degrees of freedom (DOFs) under a desired confidence level. Then, a validation matrix $\boldsymbol{\Psi}(k-1)$ is constructed in the following manner to represent the measurements that fall inside the validation regions of features:

$$\boldsymbol{\Psi}(k-1) = \left\{ \lambda_{i(k-1),t} \right\}_{(n(k-1)+1)\times T}, \quad \forall i(k-1) \text{ and } t$$

$$\lambda_{i(k-1),t} = \begin{cases} 1, & \mathbf{z}_{i(k-1)} \in Z(k-1) \text{ or } i(k-1) = 0 \\ 0, & \mathbf{z}_{i(k-1)} \notin Z(k-1) \end{cases} \tag{34}$$

where $\lambda_{i(k-1),t} = 1$ for valid measurements in the validation regions of the T features or for dummy measurements and $\lambda_{i(k-1),t} = 0$, otherwise. Using the same procedure, the set of measurements $\mathbf{Z}(k)$ (including the dummy measurements) falling inside the validation regions of features for frame k is constructed together with the validation matrix $\boldsymbol{\Psi}(k)$ and $\lambda_i(k)$

$$\mathbf{Z}(k) = \Big\{ \mathbf{z}_{i(k)} | \mathbf{v}_{i(k),t}^T \mathbf{S}_{i(k),t}^{-1} \mathbf{v}_{i(k),t} \leq g_2 \quad \forall i(k), t \Big\} \tag{35}$$

where $\boldsymbol{\Psi}(k) = \{\lambda_{i(k),t}\}_{(n(k)+1)\times T}$ $\forall i(k)$, and t, g_2 is a threshold determined from χ^2 distribution of $\dim(\mathbf{z}_{i(k)})$ DOFs under a desired confidence level, $\mathbf{v}_{i(k),t}$ denote the innovation of feature, measurement combinations at frame k, and $\mathbf{S}_{i(k),t}$ its covariance. Now, the set $\mathbf{E}_R(k)$ of association variables $\eta(t, i(k-1), i(k))$ needed to do the data association between the two frames of measurement $\mathbf{Z}(k-1)$ and $\mathbf{Z}(k)$ with the T features can be selected in the following manner:

$$\mathbf{E}_R(k) = \left\{ \eta | \lambda_{i(k-1),t} \lambda_{i(k),t} = 1 \quad \forall\, i(k-1), i(k), t \right\}. \tag{36}$$

It may be noted that the complexity of gating is $O(nm^N)$, where n is the number of features in the map and m is the number of measurements in each of the N frames. Thus, practical use of MDA with more than two frames would require recourse to special heuristics and data structures such as priority kd trees [19] for feature representation and manipulation.

D. Calculation of Log Likelihoods

Calculation of the costs $c(t, i(k-1), i(k))$ in (5) is performed by incorporating vehicle location uncertainty into the measurement model and assuming Gaussian densities for second-order statistics of the likelihoods. From (5), for two frames of measurement, there are four different cases depending on whether a feature τ_t is detected or not in the two frames.

1) When a feature $\boldsymbol{\tau}_t$ is not detected in both frames, dummy measurements $i(k-1) = 0$ and $i(k) = 0$ exist in frames $k-1$ and k, i.e., $\varepsilon(i(k-1)) = \varepsilon(i(k)) = 0$, thus, the associated cost function is

$$c(t, 0, 0) = -2\ln(1 - p_d). \tag{37}$$

2) When the feature $\boldsymbol{\tau}_t$ is detected in frame $k-1$ but not detected in frame k.: $i(k-1) \neq 0$, $i(k) = 0$, i.e., $\varepsilon(i(k-1)) = 1$ and $\varepsilon(i(k)) = 0$

$$c\left(t, i(k-1), 0\right) = -\ln\left(p_d(1-p_d) V_s L\left(\mathbf{z}_{i(k-1)} | \boldsymbol{\tau}_t\right)\right) \tag{38}$$

$$L\left(\mathbf{z}_{i(k-1)} | \tau_t\right) = \frac{\exp\left(-0.5 \mathbf{v}_{i(k-1),t}^T \mathbf{S}_{i(k-1),t}^{-1} \mathbf{v}_{i(k-1),t}\right)}{\sqrt{(2\pi)^d \det\left(\mathbf{S}_{i(k-1),t}\right)}} \tag{39}$$

where $d = \dim(\mathbf{z}_{i(k-1)})$.

3) When the feature $\boldsymbol{\tau}_t$ is detected in frame k but not detected in frame $k-1$: $i(k-1) = 0$, $i(k) \neq 0$, i.e., $\varepsilon(i(k-1)) = 0$ and $\varepsilon(i(k)) = 1$

$$c\left(t, 0, i(k)\right) = -\ln\left(p_d(1-p_d) V_s L\left(\mathbf{z}_{i(k)} | \mathbf{z}_{i(k-1)=0}, \boldsymbol{\tau}_t\right)\right) \tag{40}$$

$$L\left(\mathbf{z}_{i(k)} | \mathbf{z}_{i(k-1)=0}, \tau_t\right) = \frac{\exp\left(-0.5 \mathbf{v}_{i(k),t}^T \mathbf{S}_{i(k),t}^{-1} \mathbf{v}_{i(k),t}\right)}{\sqrt{(2\pi)^d \det\left(\mathbf{S}_{i(k),t}\right)}} \tag{41}$$

where $d = \dim(\mathbf{z}_{i(k)})$.

4) When the feature τ_t is detected in both frames $k-1$ and k: $i(k-1) \neq 0$, $i(k) \neq 0$, i.e., $\varepsilon(i(k-1)) = \varepsilon(i(k)) = 1$

$$c\left(t, i(k-1), i(k)\right) = -\ln\left((p_d V_s)^2 L\left(\mathbf{z}_{i(k-1)} | \boldsymbol{\tau}_t\right) L\left(\mathbf{z}_{i(k)} | \mathbf{z}_{i(k-1)}, \boldsymbol{\tau}_t\right)\right). \tag{42}$$

Thus, in order to calculate $c(t, i(k-1), i(k))$, we need to calculate $L(\mathbf{z}_{i(k)} | \mathbf{z}_{i(k-1)}, \boldsymbol{\tau}_t)$ as follows. Let a feature $\boldsymbol{\tau}_t$'s absolute coordinates and covariance matrix at time $k-2$ be given by $\mathbf{x}_t(k-2)$ and $\mathbf{P}_{tt}(k-2)$, respectively. Given its relative measurement $\mathbf{z}_{i(k-1)}$, corresponding measurement prediction $\widehat{z}_{i(k-1),t}$, and its uncertainty $\mathbf{P}_{i(k-1),t}$, the innovation $\mathbf{v}_{i(k-1),t}$ of feature measurement combination and its covariance matrix $\mathbf{S}_{i(k-1),t}$ can be obtained from (29)–(32). Thus, the Kalman gains $\mathbf{K}_t$ and $\mathbf{K}_v$ of the SLAM update for the feature $\boldsymbol{\tau}_t$ and vehicle pose with the measurement $\mathbf{z}_{i(k-1)}$ are given by

$$\mathbf{K}_t = \left(\mathbf{P}_{tv}(k-1|k-2)\mathbf{H}_v^T + \mathbf{P}_{tt}(k-1|k-2)\mathbf{H}_t^T\right) \times \mathbf{S}_{i(k-1),t}^{-1} \tag{43}$$

$$\mathbf{K}_v = \left(\mathbf{P}_{vv}(k-1|k-2)\mathbf{H}_v^T + \mathbf{P}_{tv}^T(k-1|k-2)\mathbf{H}_t^T\right) \times \mathbf{S}_{i(k-1),t}^{-1} \quad (44)$$

where $\mathbf{P}_{tv}(k-1|k-2)$ is the covariance prediction of feature $\boldsymbol{\tau}_t$ and $\mathbf{H}_v$ and $\mathbf{H}_t$ are the Jacobians of $\widehat{z}_{i(k-1),t}$ with respect to $\mathbf{x}_v$ and $\mathbf{x}_t$. Then, the updated position of feature $\mathbf{x}_t(k-1|k-1)$, its uncertainty, $\mathbf{P}_{tt}(k-1|k-1)$, vehicle pose $\mathbf{x}_v(k-1|k-1)$, and its uncertainty $\mathbf{P}_{vv}(k-1|k-1)$ can be calculated using the standard Kalman filter update equations. Similarly, the update of $\mathbf{P}_{tv}(k-1|k-2)$ is

$$\mathbf{P}_{tv}(k-1|k-1) = \mathbf{P}_{tv}(k-1|k-2) - \mathbf{K}_t\mathbf{S}_{i(k-1),t}\mathbf{K}_v^T. \quad (45)$$

Then, using the vehicle motion model (17), the predictions of $\mathbf{x}_v(k-1|k-1)$, $\mathbf{P}_{vv}(k-1|k-1)$, and $\mathbf{P}_{tv}(k-1|k-1)$ at time k can be computed as

$$\mathbf{x}_v(k|k-1) = \mathbf{f}\left(\mathbf{x}_v(k-1|k-1), \mathbf{u}(k-1)\right) \quad (46)$$

$$\mathbf{P}_{vv}(k|k-1) = \mathbf{F}_v\mathbf{P}_{vv}(k-1|k-1)\mathbf{F}_v^T + \mathbf{Q}_v(k) \quad (47)$$

$$\mathbf{P}_{tv}(k|k-1) = \mathbf{P}_{tv}(k-1|k-1)\mathbf{F}_v^T. \quad (48)$$

The value of $\mathbf{P}_{tt}(k-1|k-1)$ remains the same in the prediction and $\mathbf{F}_v = \partial\mathbf{f}/\partial\mathbf{x}_v$. Now, the measurement prediction $\widehat{\mathbf{z}}_{i(k),t}^*$ and its covariance $\mathbf{P}_{i(k),t}^*$ of the updated feature $\boldsymbol{\tau}_t$, the innovation with measurement $\mathbf{z}_{i(k)}$, $\mathbf{v}_{i(k),t}^*$ and its covariance $\mathbf{S}_{i(k),t}^*$ are

$$\widehat{\mathbf{z}}_{i(k),t}^* = \mathbf{h}\left(\mathbf{x}_v(k|k-1), \mathbf{x}_t(k|k-1)\right) \quad (49)$$

$$\mathbf{P}_{i(k),t}^* = \mathbf{H}_v\mathbf{P}_{vv}(k|k-1)\mathbf{H}_v^T + \mathbf{H}_t\mathbf{P}_{tt}(k|k-1)_t^{k-1}\mathbf{H}_t^T + \mathbf{H}_v\mathbf{P}_{tv}^T(k|k-1)\mathbf{H}_t^T + \mathbf{H}_t\mathbf{P}_{tv}(k|k-1)\mathbf{H}_t^T \quad (50)$$

$$\mathbf{v}_{i(k),t}^* = \mathbf{z}_{i(k)} - \widehat{\mathbf{z}}_{i(k),t}^* \quad (51)$$

$$\mathbf{S}_{i(k),t}^* = \mathbf{P}_{i(k),t}^* + \mathbf{R}(k) \quad (52)$$

where $\mathbf{H}_v$ and $\mathbf{H}_t$ are the Jacobians of $\mathbf{h}(.)$ with respect to $\mathbf{x}_v(k|k-1)$ and $\mathbf{x}_t(k|k-1)$. Now, the likelihood of $\mathbf{z}_{i(k)}$ given $\mathbf{z}_{i(k-1)}$ and $\boldsymbol{\tau}_t$ is given by (53) with $d = \dim(\mathbf{z}_{i(k)})$ as

$$L\left(\mathbf{z}_{i(k)}|\mathbf{z}_{i(k-1)}, \boldsymbol{\tau}_t\right) = \frac{\exp\left(-0.5\left(\mathbf{v}_{i(k),t}^*\right)^T\left(\mathbf{S}_{i(k),t}^*\right)^{-1}\left(\mathbf{v}_{i(k),t}^*\right)\right)}{\sqrt{(2\pi)^d \det\left(\mathbf{S}_{i(k),t}^*\right)}}. \quad (53)$$

Now, the data-association problem in SLAM can be solved in the form of a linear programming problem. In this study, an efficient and much faster interior-point algorithm known as Mehrotra's predictor corrector method [12] having a polynomial complexity is used to solve the resulting linear program as detailed in Section II.

IV. Algorithm Performance

A. Performance Evaluation

The performance of the MDA data-association algorithm for two frames of measurement in EKF SLAM was extensively evaluated in a simulated environment. The feature measurements are assumed to be from a scanning range measurement system such as a SICK LMS 290. The control input to the vehicle kinematic model is assumed to be from steering and wheel encoders.

$\Psi(k-1) =$

	1	2	3	4	5	
	1	1	1	1	1	0
	1	0	0	0	0	1
	0	1	0	0	0	2
	0	0	1	0	0	3
	0	0	0	1	0	4
	0	0	0	0	1	5
	1	0	0	0	0	6

$\Psi(k) =$

	1	2	3	4	5	
	1	1	1	1	1	0
	1	0	0	0	0	1
	0	1	0	0	0	2
	0	0	1	0	0	3
	0	0	0	1	0	4
	0	0	0	0	1	5
	0	1	0	0	0	6
	0	0	0	0	1	7
	0	0	1	0	0	8
	0	0	0	0	0	9

Fig. 1. Validation matrices for the association hypotheses. The columns in validation matrices consist of available features and rows correspond to the measurements in respective frames.

Scenario I: Illustration of MDA in SLAM: First, to illustrate the operation of MDA in EKF SLAM, a simple scenario is considered. The vehicle is assumed to be traveling in a 20-m-radius circular path in an environment consisting of ten randomly generated features. The spurious measurements are assumed to be uniformly distributed in the environment, and their returns are Poisson distributed [4]. The simulation specific parameters are: speed input error of 0.5 m/s, steering angle encoder error of 0.05 rad, range measurement noise of 0.1 m, maximum range of 20 m, bearing measurement error of 0.5°, and spurious measurement or clutter density of 0.02 m^{-2}.

Fig. 1 shows an association scenario at a particular instant ($k = 15$) with five features in the state vector. The number of spurious measurements in the preceding frame $k-1$th (14th) and current kth frame (15th) are 1 and 4, respectively, and the number of true measurements in both frames is 5. For this state of affairs, the validation matrices of the two consecutive frames are as shown in Fig. 1. At this instant, there are, in all, 28 hypotheses corresponding to the different combinations of the measurements of the two frames and the features in the state vector. It is seen from Fig. 2 that for correct measurement-to-feature associations, the association variables evaluate to 1 and incorrect assignments to negligibly small values. The association probability in Fig. 2 is the value of the association variable as determined by the solutions to the algorithm, which is between 0 and 1.

Scenario II: High Spurious Measurements in a Static Environment: The following simulation demonstrates the MDA algorithm's performance in SLAM when there is a significant proportion of spurious measurements (that may be due to the nature of environment, or poor sensor performance, or both) and higher feature density. This scenario is quite demanding for any data association scheme. Here, the vehicle is assumed to be traveling in a manually generated path (Fig. 3) in a 100×100 m^2 area environment, consisting of 100 randomly generated static features. The spurious measurement spread and the noise parameters used are as given in the first example. Figs. 4

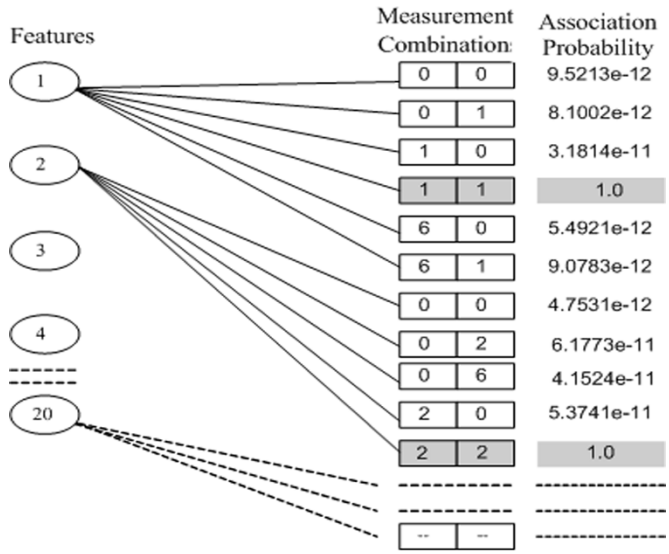

Fig. 2. Feature-to-measurement association hypotheses. The figure shows possible association hypothesis in one instant. Measurement combinations shown in squares indicate the measurement indexes in two consecutive frames of measurements.

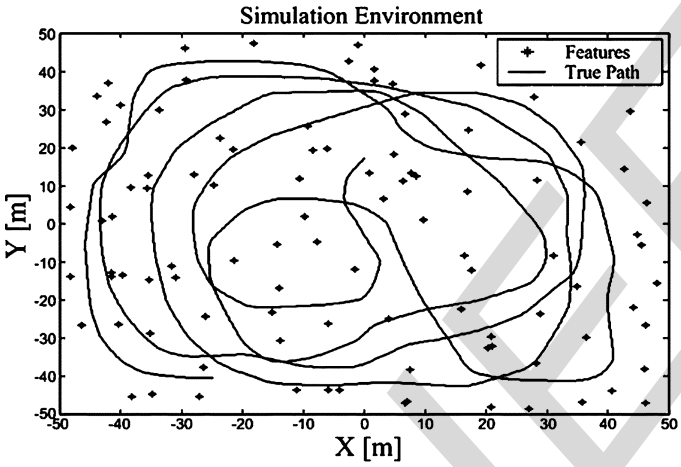

Fig. 3. Simulated environment. The crosses represent the location of the map features. The true trajectory of the robot is shown by the thick line.

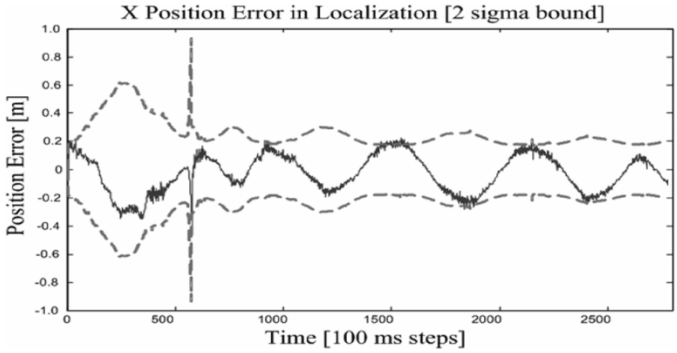

Fig. 4. Lateral position error in SLAM with two-frame data association. Estimated 2 sigma bounds of the localization error are shown by the dashed lines.

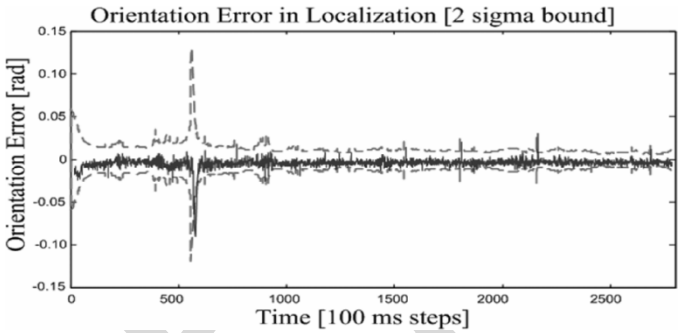

Fig. 5. Orientation error in SLAM with two-frame data association. Estimated 2 sigma bounds of the localization error are shown by the dotted lines.

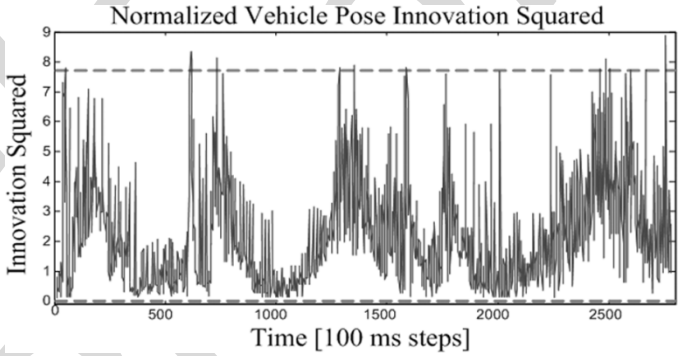

Fig. 6. Normalized vehicle pose ($[x(k)\ y(k)\ \theta(k)]^T$) innovation squared plot of the SLAM implementation with two-frame data association. Chi-square 95% confidence limits of 3 DOFs for normalized innovation squared are shown by the dashed lines.

and 5 show that the error bounds for position (only lateral position error is shown) and orientation are well within the 2σ limits, demonstrating the effectiveness of the MDA data association in EKF SLAM. The MDA data-association filter's consistency is clearly seen from the plot of normalized vehicle pose ($[x(k)\ y(k)\ \theta(k)]^T$) innovation squared versus time shown in Fig. 6. It is apparent from the results that the performance of SLAM with MDA data association is good even under high spurious measurement density and high feature density.

The MDA data-association scheme in EKF-SLAM is compared with the standard NN data-association filter and JCBB by performing several Monte Carlo runs under the same conditions using the same set of simulation parameters. A good measure of performance of data association in this case is the percentage of missed associations or percentage track loss measure [20], which is the ratio of missed associations to total observed instances of a feature expressed as a percentage. Fig. 7 depicts the percentage of missed associations (i.e., features left unassociated or associated with another feature) of the various methods with varying densities of spurious measurement. Fig. 7 also shows that the performance of data association in SLAM is significantly improved with MDA with two frames, compared with the standard NN data association, especially in high densities of spurious measurement. The MDA algorithm's performance is comparable to that of JCBB at lower densities of spurious measurement. However, with increasing densities of spurious measurement, there is a marked improvement in performance of MDA over JCBB.

Scenario III: In the Presence of Moving Objects: This scenario evaluates the robustness of MDA to temporarily persistent

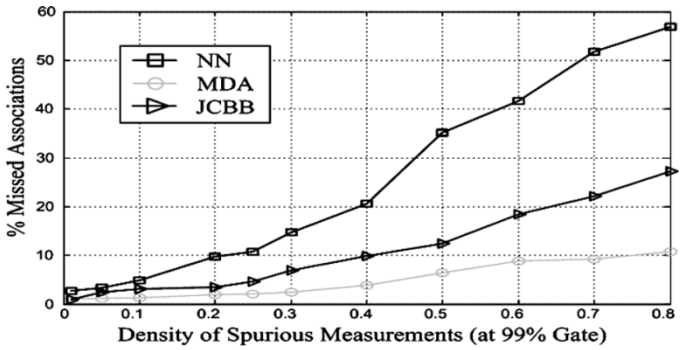

Fig. 7. Percentage of missed associations versus density of spurious measurements.

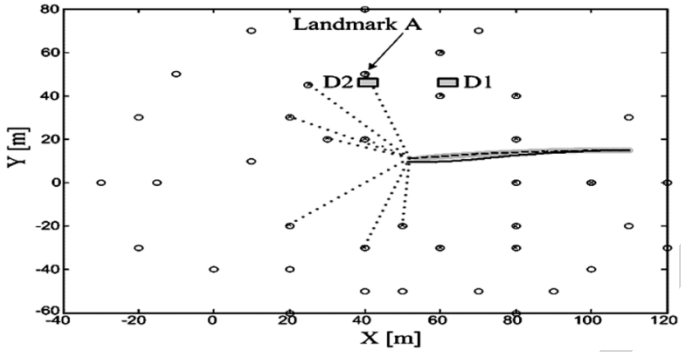

Fig. 8. Performance of data-association algorithms in a dynamic setting. The thick, thin, and dotted lines represent true robot trajectory, trajectory due to odometry, and the estimated robot trajectory. Big shaded squares represent the dynamic objects. Circles represent true landmark positions and crosses represent estimated landmark positions. Dotted lines connecting the robot and landmarks indicate that this particular landmark generates a measurement.

dynamic clutter that may be due to moving objects or objects of varying sizes in the environment. The first dynamic scenario is considered to provide insight into MDA's ability to remove temporarily persistent clutter due to moving objects in the environment. This involves a vehicle navigating and performing SLAM in an environment consisting of several landmarks. An object travels through this environment at constant speed, as shown in the Fig. 8. Assume that at time $k = 148$ (14.8 s), the static landmark A has already been initialized into the map and has been observed by the robot's sensors at $k = 147$ (14.7 s). The dynamic object is at D1 at this instance. Now, the vehicle receives a measurement M1 from the landmark A. Under these circumstances. all data-association schemes NN, JCBB, and MDA correctly associate M1 with A. At $k = 149$ (14.9 s), the dynamic object moves left and stops at D2. Now, the landmark A is occluded and thus no measurement is received from landmark A or from the dynamic object. Thus, NN, MDA, and JCBB correctly conclude that the landmark A is not observed. At $k = 150$ (15 s), the dynamic object still remains at D2. However, the vehicle moves to the left, causing its sensors to receive a spurious measurement M2 due to the dynamic object. In this instance, both NN and JCBB wrongfully conclude that landmark A is observed and associate it with M2. Nevertheless, two-frame MDA correctly concludes that M2 is a spurious measurement as it is not observed at k =149 (14.9 s). This scenario illustrates how

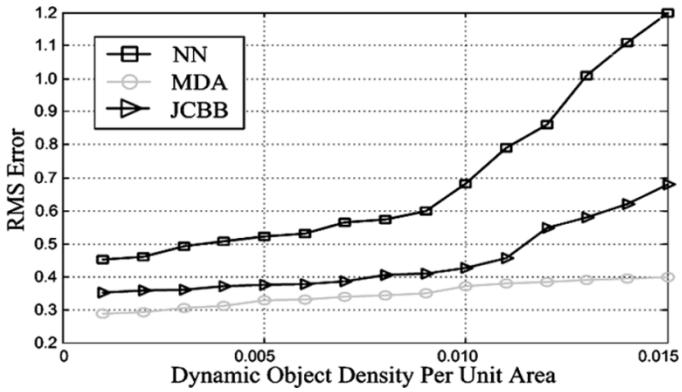

Fig. 9. Comparison of rms error in X in a dynamic setting.

the multiple-frame data-association schemes such as MDA have the potential to filter out dynamic objects and persistent clutter.

In the final simulation scenario, we evaluate the performance of the three algorithms when carrying out SLAM in a more realistic dynamic environment (Fig. 3), i.e., in the presence of many moving objects such as people, vehicles, or other nonstatic objects. A dynamic or moving object's motion is modeled using a Brownian motion model [where the velocity of the object $\mathbf{v}(k)$ at time k is given by $\mathbf{v}(k+1) = \mathbf{v}(k) + \mathbf{n}(k)$, where $n(k) \sim N(0, Q_n)$], i.e., the velocity of the moving object is subject to random perturbations. The number of dynamic objects at a given instance is obtained from a Poisson distribution whose density is varied from 0.001/m^2 to 0.015/m^2. A uniform probability density function (pdf) is used to initialize the position, and a Gaussian pdf is used to initialize the speed of an object. The noise parameters of Scenario I is used here. Fig. 9 shows the vehicle's X-position root mean square (rms) error measure with MDA, JCBB, and NN data-association methods in SLAM. It is seen that MDA clearly outperforms both JCBB and NN.

Although JCBB tests compatibility of groups of measurements in the current time frame, thereby dealing with the spatial correlations in the present time frame, it lacks the ability to filter out temporal correlations over several time frames. On the other hand, MDA removes spurious measurements or returns due to dynamic objects by checking for consistency of measurement-to-feature associations over several consecutive frames. Therefore, MDA is able to deal with dynamic objects and temporarily persistent clutter by including more than one frame of measurement in the process. This enables the MDA to filter out the spurious measurements resulting from the dynamic objects.

B. Complexity and Computational Efficiency

The complexity of the linear program can be reduced significantly by the preprocessing steps described in Section III. The linear program solution to the assignment problem is obtained by a primal-dual infeasible interior-point approach known as Mehrotra's predictor corrector method [12]. Methods that generate iterations lying in the interior of the feasible set (rather than on the boundary, as simplex methods do) such as Mehrotra's predictor corrector method were first proposed by Karmarkar [21]. Karmakar's method has proved to be several times faster than the simplex algorithm and made it possible to solve many

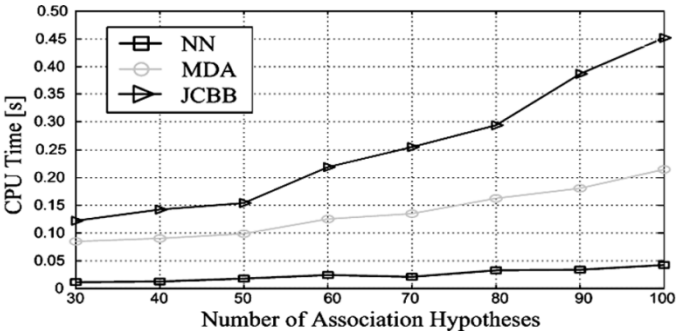

Fig. 10. Comparison of average computational load.

large linear programming problems (e.g., a military aircraft optimal route-selection problem with variables and constraints in the order of 10^5 and 10^4, respectively) which required a prohibitively large amount of computer resources when solved by the simplex algorithm. It can be shown that, for the two-frame 3-D data-association method with the preprocessing functions applied in SLAM, a worst case complexity that grows with the cube of the number of association hypotheses is achieved.

In this study, several studies were conducted to compare the actual computation time required by MDA, the standard NN, and JCBB in SLAM. The CPU time requirement for the preprocessing and data-association functions are determined using several Monte Carlo runs by using a Pentium 4 2.4-GHz, 512-MB RAM PC and is given in Fig. 10.

Of the three, the computation time for JCBB is the highest. Although the computation time for MDA is much higher than for NN, it is still feasible for real-time implementation in EKF-SLAM. The computation time of MDA can be appreciably reduced with better preprocessing of the features before association, thereby further reducing the number of association variables.

C. Experimental Results

The experimental verification of the MDA data association in EKF-SLAM is conducted using an in-house-built autonomous vehicle shown in Fig. 11. The sensors onboard the vehicle, amongst others, include a SICK LMS 290 laser measurement system, a fiber-optic gyroscope (FOG) [Hitachi HOFG 1(A)], rear and front wheel optical encoders (IE 58), and a steering encoder (GI 338). The SICK LMS 290 provides range measurements to objects ahead at 1° intervals over a span of 180° in one scan. The scanned data arriving at 0.1-s intervals from this range measurement system is segmented and clustered as in [22] to extract features. The outputs of the wheel and steering encoders are used as inputs to the vehicle kinematic model for vehicle pose prediction. The output of the FOG is also used as a vehicle orientation measurement. Features extracted from the laser and the measurements from encoders are then used to implement the EKF-SLAM with the particular data-association scheme.

In the first experiment, the performance of the MDA filter in SLAM is evaluated when the vehicle is moving in a small-sized loop in a mainly static environment. The vehicle is driven at an average speed of about 3 m/s along an approximately 170-m

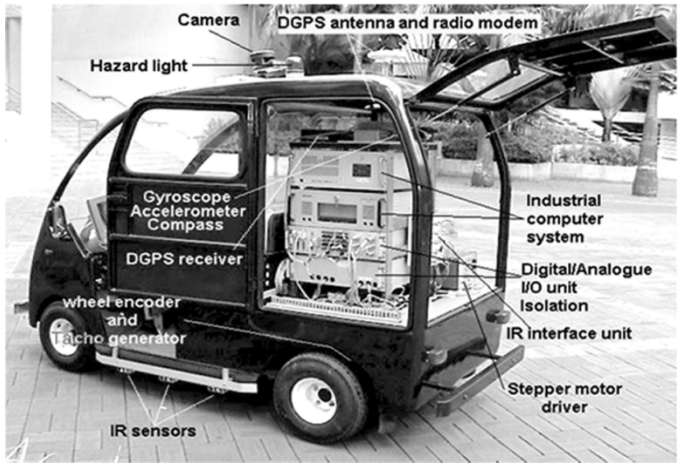

Fig. 11. Mobile robot used in SLAM experiments.

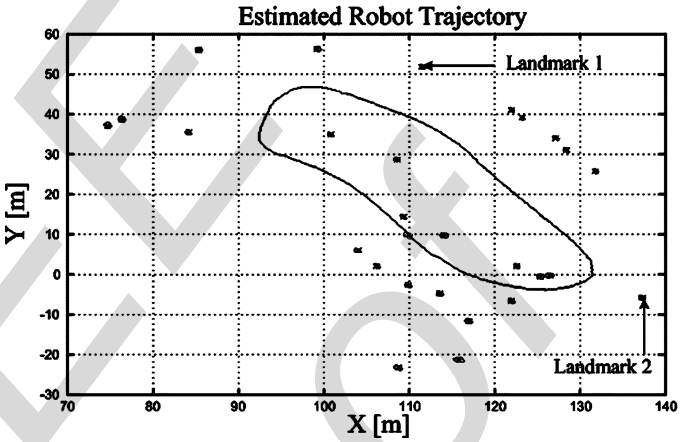

Fig. 12. Estimated vehicle path (thick line) and feature locations (circles) (SLAM experiment in a campus car park).

stretch of road in a 60×60 m^2 area car park on campus. The mapped feature (lamp posts and tree trunks) locations and vehicle-path estimates obtained using EKF SLAM with MDA data association for a specific trial are as shown in Fig. 12. It is observed that the extracted features per scan vary from about 0 to 35 with an average of 18. The plot of the range-measurement innovation metric is used to measure the data-association filter consistency. As shown in Fig. 13, the range innovation plot is well within the 2σ bounds, thus demonstrating the MDA filter's consistency. A measure of ground truth of map estimation accuracy is obtained by comparing the estimated positions with ground truth of several artificial landmarks, viz. fiberglass posts placed at known locations with respect to the origin of the global reference frame chosen arbitrarily to be the vehicle starting position. Figs. 14 and 15 show the true errors of MDA for the known artificial landmarks 1 and 2 shown in Fig. 12. The actual feature estimation errors are bounded within the 2σ limits, further demonstrating the effectiveness and consistency of the MDA filter.

The actual loop-closing error is used as a measure of vehicle path accuracy. This error is measured by starting the vehicle at a marked location and stopping at the same place after

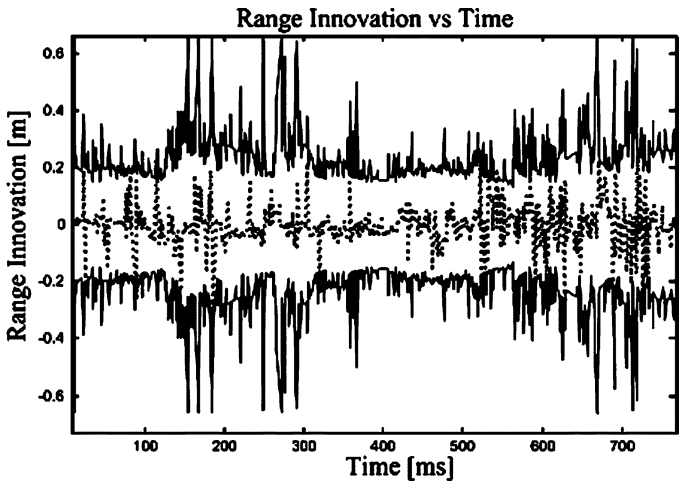

Fig. 13. Filter performance: range innovation (dotted line) and its two sigma bounds (thick line).

traversing a loop and running offline runs on the data sets collected. The loop closing error, which is the Euclidian distance from the starting and estimated ending positions obtained, is within 0.6 m over the 170-m length stretch. The improvement in loop closing error of MDA over NN is about 8.3% and, as against JCBB, it is 4.1%. Fig. 16 shows the computation times for MDA, JCBB, and NN data-association algorithms. It may be noted that the computation time for NN is the least. Although the computation time of MDA is higher than that for the NN, it is consistent with real-time requirements. The computation time for JCBB, as expected, is higher and is very significant, especially with increasing spurious measurements and many features. As illustrated in the plot of Fig. 16, the increased computational requirements of JCBB is due to the variable but large number of traversals of the hypothesis tree required at each time step by the joint compatibility algorithm, even with branch and bound pruning. This shows that implementing a JCBB can be quite challenging from a computational perspective with a large number of spurious measurements and feature densities, which is typical of many outdoor environments, and for poor sensor and feature extraction. However, the number of hypotheses traversed by the MDA does not show an excessive variation like in JCBB for the same experimental conditions (see Fig. 17), although the results are marginally better than the JCBB.

An experiment was then conducted in a larger static outdoor environment to test MDA's robustness in the presence of propagating nonlinearities inevitable in large-scale SLAM. The vehicle is driven at an average speed of 4 m/s along an approximately 1-km stretch of road on the campus. A digital map (scale 1:5000) of the area of interest is shown in Fig. 18. In this experiment, it is observed that the number of features extracted varies from zero to 55 with an average of 27. The results of the estimated vehicle path ($\approx$1 km) and the feature locations are shown superimposed on the digital map in Fig. 18 for SLAM using MDA data association. From Fig. 18, it may be seen that there is an approximate loop-closing error of 12.5 m. The closure error for JCBB and NN are, respectively, 15% (15.2 m) and 28% (16 m), which is more in relation to MDA. These results show that MDA is more robust and accurate than both NN and JCBB in large outdoor spaces where spurious measurements are quite high. Although sizable, the relatively small values of the loop-closing errors (considering the loop size) of all three algorithms are mainly due to the good accuracy of the FOG and odometry. However, in all three cases, it was not possible to match the features detected at the start of the journey with the same detected at the end while completing the loop. This inability to remap features when completing the loop and the sizable loop-closing error are due to propagating nonlinearities inherent in the EKF in large-scale SLAM, observability issues, as well as the data-association errors. The difference in data-association filter performances is partly why the loop-closing error results obtained for each of the methods for the same data sets are different.

Finally, the robustness of MDA in dynamic environments is experimentally evaluated from data sets collected from a busy campus car park where moving vehicles and people are observed during the experiment. EKF SLAM was run for data sets using NN, MDA, and JCBB algorithms, and the loop-closing error was measured. The estimated trajectories for a particular but typical data set are shown in Fig. 19. The MDA, JCBB, and NN algorithms result in a loop-closing error of 1.5, 1.9, and 2.2 m, respectively, on the average over a distance of 350 m. Thus JCBB and NN result in a 27% and 47% increase in the loop-closing error when compared with that of MDA in dynamic environments where static environment assumption of the standard SLAM is violated. This marked improvement of MDA's performance and robustness over the NN and JCBB methods in this particularly dynamic scenario can be attributed to the use of more than one frame of measurement in MDA in the data-association process, thus providing means of removing the returns due to moving objects and spurious measurements, as was explained through simulations in Scenarios 1 and 3 in Section IV-A.

V. Discussion

The MDA algorithm works fairly well in general outdoor settings with trees, lamp posts, and other rigid structures in the environment. Under very poor feature extraction and scarcity of features, the performance of the MDA degrades due to increasing vehicle uncertainty, which is unavoidable as with any other scheme. For example, when the vehicle is operating in an area populated with dense vegetation consisting of stunted trees and bushes, the simple feature extraction methodology based on the centroid of regions of constant depth used here becomes inadequate. In areas sparsely populated with prominent features, the measurements obtained are few and far between, causing very significant vehicle uncertainty between updates, resulting in degraded performance.

Since the MDA problem, which is a nonlinear 0–1 integer programming problem, is solved through relaxation of the integer constraint on the association variables, the data association is occasionally suboptimal. This means that, although very rare, there can be occasions where the association variables may evaluate to fractional values, necessitating appropriate handling. One approach is to interpret the resulting fractional solutions

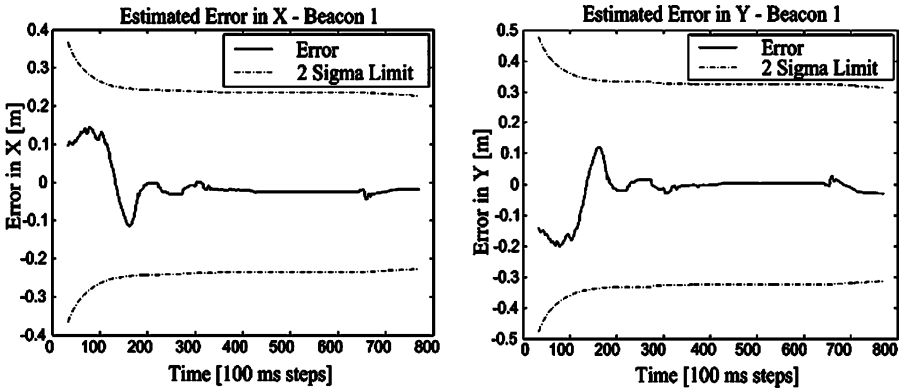

Fig. 14. Difference between the actual and estimated location for landmark 1. The 95% confidence limit is shown by dotted lines.

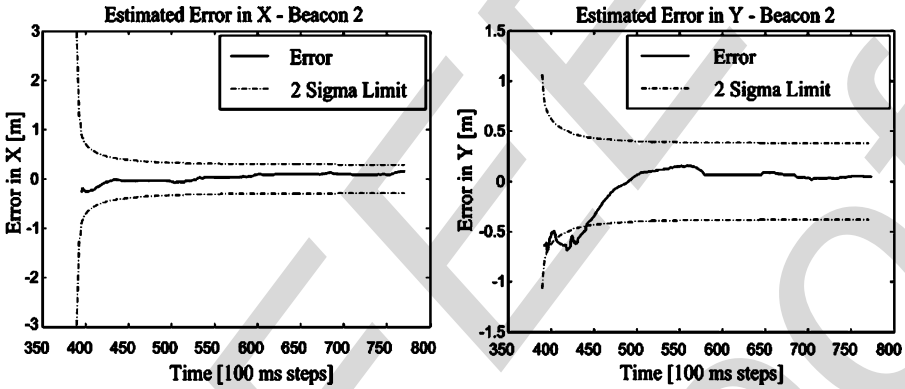

Fig. 15. Difference between the actual and estimated location for landmark 2. The 95% confidence limit is shown by dotted lines.

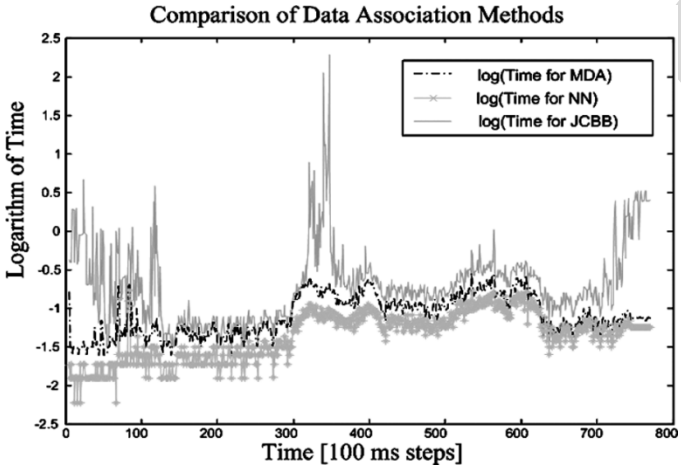

Fig. 16. Comparison of the time complexity of data-association algorithms. Time is shown for data sampled at 0.1 s in the actual experiment.

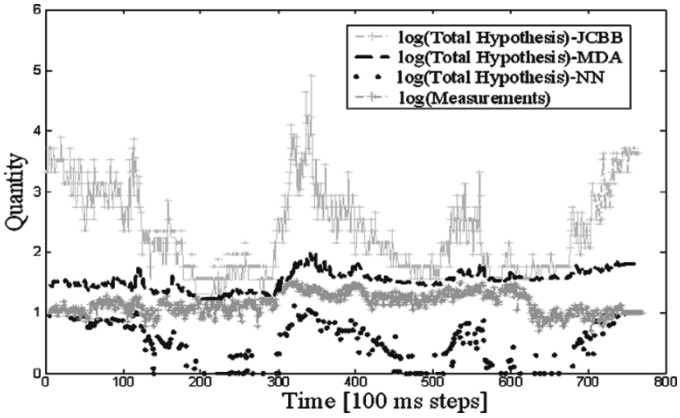

Fig. 17. Comparison of number of association hypotheses traversed.

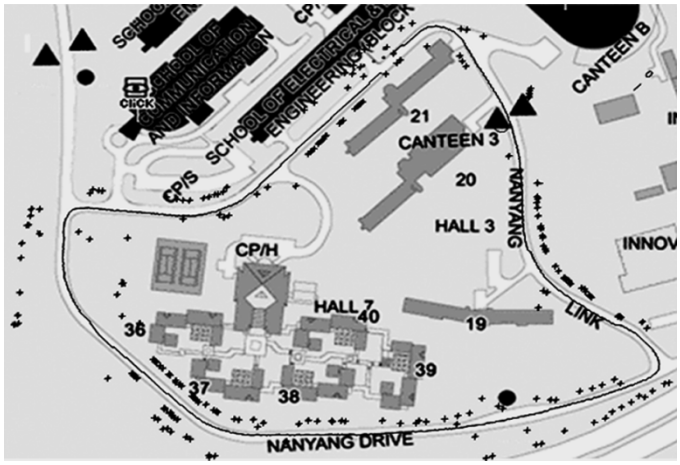

Fig. 18. Large-scale SLAM experiment performed in a university campus environment. The estimated vehicle path is shown by the thick line and features are shown by crosses.

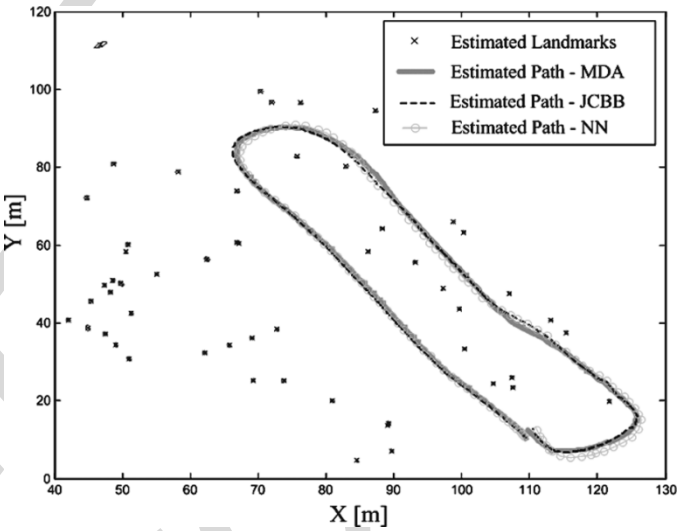

Fig. 19. Robustness to dynamic environments. The map is shown with the MDA data association (for clarity). The estimated robot trajectories are shown for NN, MDA, and JCBB data-association algorithms.

for the association variables η as association probabilities specifying the correspondence between feature $\boldsymbol{\tau}_t$ and the measurement $\mathbf{z}_{i(k)}$. Let $w_{i(k),t} = \sum_{i(k-1)=0}^{n(k-1)} \eta(t, i(k-1), i(k))$. Then, from (10), we have $\sum_{i(k)=0}^{n(k)} \sum_{i(k-1)=0}^{n(k-1)} \eta(t, i(k-1), i(k)) = 1$ for all $\mathrm{t} = 1, 2, \ldots, T$. Thus, $\sum_{i(k)=0}^{n(k)} w_{i(k),t} = 1$ for $t = 1, 2, \ldots, T$.

During such instances, a JPDA type of update is utilized [20] in the state update process, by modifying the EKF estimation equations where necessary as follows:

$$\mathbf{v}_{i(k)} = \mathbf{z}_{i(k)} - \widehat{\mathbf{z}}_{i(k)} \tag{54}$$

$$\overline{\mathbf{v}}(k) = \sum_{i(k)=0}^{n(k)} w_{i(k),t} \mathbf{v}_{i(k)} \tag{55}$$

$$\mathbf{X}(k|k) = \mathbf{X}(k|k-1) + \mathbf{K}(k)\overline{\mathbf{v}}(k) \tag{56}$$

$$\mathbf{P}(k|k) = w_{0,t}\mathbf{P}(k|k-1) + (1 - w_{0,t})\mathbf{P}^*(k) + \mathbf{K}(k)\mathbf{W}^*(k)\mathbf{K}^T(k) \tag{57}$$

$$\mathbf{P}^*(k) = (\mathbf{I} - \mathbf{K}(k)\mathbf{H}(k))\,\mathbf{P}(k|k-1) \tag{58}$$

$$\mathbf{W}^*(k) = \sum_{i(k)=0}^{n(k)} \left(w_{i(k),t} \overline{\mathbf{v}}(k) \mathbf{v}_{i(k)}^T - \overline{\mathbf{v}}(k) \mathbf{v}_{i(k)}^T \right) \tag{59}$$

where $\mathbf{K}(k)$ is the Kalman gain, $\widehat{z}_{i(k)}$ is the predicted value of the observation $\mathbf{z}_{i(k)}$, and $\mathbf{H}(k)$ is the Jacobian of $\widehat{z}_{i(k)}$ with respect to $\mathbf{X}(k)$.

Solving the data-association problem as a multidimensional assignment problem is subject to the constraints that each measurement can be associated with, at most, one feature in the map, and a map feature can be associated with, at most, one measurement in a frame. This can be a limiting assumption in certain applications in the choice of features or representation of features.

VI. Conclusion

A generalized, nonlinear, optimization-based framework for data association is established. It is shown how different data-association algorithms, including the most common single-frame-of-measurement-based NN and multiple-measurement-frames-based optimal MHT methods and its variants can be synthesized by an appropriate choice of the cost function. More specifically, a multimeasurement-frame association methodology is then derived based on MDA for SLAM by using the joint likelihood of measurements in multiple frames and features as the cost function. MDA-based data association using two frames of measurement is rigorously formulated for concurrent robot localization and mapping by incorporating the sensor location uncertainty. The MDA-based algorithm is a practical and effective alternative to the theoretically optimal MHT. Compared with single-measurement-frame methods, the MDA resolves association incompatibilities and ambiguities more effectively and yields consistent maps, especially with increased spurious measurements (clutter) and feature density and in the presence of moving objects. In particular, this study establishes that even though the complexity of two-frame data association is higher, it significantly outperforms standard NN data association. As compared with JCBB, which takes full account of the spatial correlations between vehicle and features in a single frame, MDA does better in settings with very high spurious measurement densities and in the presence of moving

objects. In addition, MDA is more efficient computationally and amenable to real-time implementation, unlike JCBB, despite JCBC's use of branch-and-bound pruning of its exponential search space. This is especially so in dynamic environments with high spurious measurement densities.

When clutter is high and features are sparse, the compatibility information of features of a single measurement frame is not sufficient to make effective data-association decisions, thus compromising performance of single-frame-based methods. However, in a multiple-measurement-frame approach, the availability of more than one frame of measurement provides for more effective data-association decisions as consistency of measurements are looked at in several frames of measurement. This is particularly why the performance of MDA shows a marked improvement over other schemes in high clutter and in the presence of dynamic objects. Moreover, the MDA algorithm can be readily deployed using standard PC computing resources in real time without any custom processing hardware. This is primarily due to the polynomial time complexity of the primal-dual infeasible interior-point approach, which is used to obtain a suboptimal solution to the 0–1 integer-programming problem of multidimensional assignment.

Another major advantage of the proposed MDA-based data-association technique is that it can be a practical alternative to the optimal MHT-based data association if a moving window involving many (>2) measurement frames is utilized. The NP-hard MHT-based data association can become intractable due to combinatorial explosion in dense feature and clutter scenarios. The solution of MDA-based data association involving more than two frames is computationally tractable with a multistage Lagrangian relaxation approach and use of appropriate data structures. Therefore, this type of MDA-based data-association algorithm, employing a finite sliding window, can prove to be advantageous over the other deferred logic approaches in every domain. Moreover, robust data-association schemes such as this would definitely contribute toward developing localization and mapping algorithms with less reliance on efficient and effective feature extraction methods.

APPENDIX I

Data association using two frames of measurement is given as follows:

$$\Lambda_{\text{false}}(\Omega)=\left(\frac{1}{V_s}\right)^{n(k-1)-T(k-1)}\left(\frac{1}{V_s}\right)^{n(k)-T(k)} \tag{60}$$

$$\begin{aligned}\Lambda_{\text{true}}(\Omega)=&\prod_{\forall t}\left(p_d L\left(\mathbf{z}_{i(k-1)}|\boldsymbol{\tau}_t\right)\right)^{\varepsilon(i(k-1))}\\&\times\left(1-p_d\right)^{1-\varepsilon(i(k-1))}\\&\times\left(p_d L\left(\mathbf{z}_{i(k)}|\mathbf{z}_{i(k-1)},\boldsymbol{\tau}_t\right)\right)^{\varepsilon(i(k))}\\&\times\left(1-p_d\right)^{1-\varepsilon(i(k))}\end{aligned} \tag{61}$$

$$\Lambda_N(\Omega)=\frac{\Lambda_{\text{false}}(\Omega)\Lambda_{\text{true}}(\Omega)}{\left(V_s^{-n(k)}V_s^{-n(k-1)}\right)} \tag{62}$$

$$\Xi(\Omega)=-\ln\left(\Lambda_N(\Omega)\right)=\sum_{\Omega}c(t,i(k-1),i(k))\,. \tag{63}$$

The optimal association is then the solution to

$$\begin{aligned}\text{Minimize}\sum_{i(k-1)=0}^{n(k-1)}\sum_{i(k)=0}^{n(k)}\sum_{t=1}^{T}&\eta\left(t,i(k-1),i(k)\right)\\&\times c\left(t,i(k-1),i(k)\right)\end{aligned} \tag{64}$$

subject to the following constraints:

$$\sum_{i(k)=0}^{n(k)}\sum_{t=1}^{T}\eta\left(t,i(k-1),i(k)\right)\le 1,\quad i(k-1)=1,2,\ldots,n(k-1) \tag{65}$$

$$\sum_{i(k-1)=0}^{n(k-1)}\sum_{t=1}^{T}\eta\left(t,i(k-1),i(k)\right)=1,\quad i(k)=1,2,\ldots,n(k) \tag{66}$$

$$\sum_{i(k-1)=0}^{n(k-1)}\sum_{i(k)=0}^{n(k)}\eta\left(t,i(k-1),i(k)\right)=1,\quad t=1,2,\ldots,T \tag{67}$$

$$\sum_{i(k)=0}^{n(k)}\sum_{t=1}^{T}\eta_1\left(t,0,i(k)\right)\le T \tag{68}$$

$$\sum_{i(k-1)=0}^{n(k-1)}\sum_{t=1}^{T}\eta\left(t,i(k-1),0\right)\le T \tag{69}$$

$$\eta=\{0,1\}\ \forall i(k-1),\quad i(k),\ t=1,2,\ldots,T. \tag{70}$$

REFERENCES

[1] R. Smith, M. Self, and P. Cheeseman, "A stochastic map for uncertain spatial relationships," in *Proc. 4th Int. Symp. Robot. Res.*, 1987, pp. 467–474.

[2] J. J. Leonard and H. F. Durrant-Whyte, "Mobile robot localization by tracking geometric beacons," *IEEE Trans. Robot. Autom.*, vol. 7, no. 3, pp. 376–382, Jun. 1991.

[3] M. W. M. G. Dissanayake, P. Newman, S. Clark, H. F. Durrant-Whyte, and M. Csorba, "A solution to the simultaneous localization and map building (SLAM) problem," *IEEE Trans. Robot. Autom.*, vol. 17, no. 3, pp. 229–241, Jun. 2001.

[4] Y. Bar-Shalom and T. E. Fortman, *Tracking and Data Association*. Orlando, FL: Academic, 1988, vol. 179, Mathematics in Science and Engineering.

[5] D. B. Reid, "An algorithm for tracking multiple targets," *IEEE Trans. Autom. Control*, vol. AC-24, no. 6, pp. 843–854, Dec. 1979.

[6] C. L. Morefield, "Application of 0–1 integer programming to multitarget tracking problems," *IEEE Trans. Autom. Control*, vol. AC-22, no. 3, pp. 302–312, Jun. 1977.

[7] A. B. Poore and A. J. Robertson, "A new multidimensional data association algorithm for multisensor multitarget tracking," *Proc. SPIE*, vol. 2561, pp. 448–459, Jul. 1995.

[8] S. Deb, K. R. Pattipati, B. S. Yaakov, and M. Yeddanapudi, "A generalized S-D assignment algorithm for multisensor-multitarget state estimation," in *Proc. 33rd Conf. Decision Control*, Lake Buena, FL, Dec. 1994, pp. 3293–3298.

[9] X. Li, Z. Q. Luo, K. M. Wong, and E. Bosse, "An interior point linear programming approach to two-scan data association," *IEEE Trans. Aerosp. Electron. Syst.*, vol. 35, no. 2, pp. 474–490, Apr. 1999.

[10] A. Doucet, N. de Freitas, K. Murphy, and S. Russell, "Rao-Blackwellised particle filters for dynamic Bayesian networks," in *Proc. Uncertainty in AI*, 2000, p. XXX ***[Author: Please provide page numbers.--Ed.]***.

[11] M. Montemerlo, S. Thrun, D. Koller, and B. Wegbreit, "FastSLAM: A factored solution to the simultaneous localization and mapping problem," in *Proc. AAAI Nat. Conf. Artif. Intell.*, Edmonton, AB, Canada, 2002, pp. XXX–XXX***[Author: Please provide page numbers.--Ed.]***.

[12] Y. Zhang, Solving Large Scale Linear Programs by Interior Point Methods Under MATLAB Environment Dept. Math. and Statistics, Univ. Maryland, Baltimore, MD, Tech. Rep. TR96-01, Jul. 1995.

[13] T. Baily, "Mobile robot localization and mapping in extensive outdoor environments," Ph.D. dissertation, Australian Centre for Field Robotics, Dept. Aerosp., Mech. Mechatron. Eng., Univ. of Sydney, Sydney, Australia, Aug. 2002.

[14] S. Blackman and R. Popoli, *Design and Analysis of Modern Tracking Systems*. Boston, MA: Artech House, 1999.

[15] J. Dezert and Y. Bar-Shalom, "Joint probabilistic data association for autonomous navigation," *IEEE Trans. Aerosp. Electron. Syst.*, vol. 29, no. 4, pp. 1275–1286, Oct. 1993.

[16] D. Maksarov and H. Durrant Whyte, "Mobile vehicle navigation in unknown environments: A multiple hypothesis approach," *Proc. IEE Control Theory Appl.*, vol. 142, no. 4, pp. 385–400, Jul. 1995.

[17] J. E. Guivant and E. Nebot, "Optimization of the simultaneous localization and map-building algorithm for real-time implementation," *IEEE Trans. Robot. Autom.*, vol. 17, no. 3, pp. 242–257, Jun. 2001.

[18] J. J. Leonard and H. J. S. Feder, "Decoupled stochastic mapping," *IEEE J. Ocean. Eng.*, vol. 26, no. 4, pp. 561–571, Oct. 2001.

[19] J. K. Uhlmann, "Dynamic map building and localization: New theoretical foundations," Ph.D. dissertation, Robot. Res. Group, Dept. Eng. Sci., Oxford Univ., Oxford, U.K., 1995.

[20] H. Chen, T. Kirubarajan, and Y. Bar-Shalom, "Tracking of spawning targets with multiple finite resolution sensors," in *Proc. 5th Int. Conf. Inf. Fusion*, Annapolis, MD, 2002, vol. 2, pp. 943–950.

[21] N. Karmarkar, "A new polynomial-time algorithm for linear programming," *Combinatorica*, vol. 4, pp. 373–395, 1984.

[22] J. E. Guivant, F. R. Mason, and E. M. Nebot, "Simultaneous localization and map building using natural features and absolute information," *Robot. Auton. Syst.*, vol. 40, pp. 79–90, Aug. 2002.

[23] J. Neira and J. D. Tardos, "Data association in stochastic mapping using the joint compatibility test," *IEEE Trans. Robot. Autom.*, vol. 17, no. 6, pp. 890–897, Dec. 2001.

[24] D. Haehnel, W. Burgard, B. Wegbreit, and S. Thrun, "Toward lazy data association in SLAM," in *Proc. 11th Int. Symp. Robot. Res.*, Sienna, Italy, 2003***[Author: Please provide page numbers.--Ed.]***.

[25] J. Nieto, J. Guivant, E. Nebot, and S. Thrun, "Real time data association for FastSLAM.," in *Proc. IEEE Int. Conf. Robot. Autom.*, Taipei, Taiwan, R.O.C., Sep. 14–19, 2003, pp. 412–418.

W. Sardha Wijesoma (M'99) received the BSc. Engineering Hons. degree in electronics and telecommunication engineering from the University of Moratuwa, Moratuwa, Sri Lanka, in 1983, and the Ph.D. degree in robotics from Cambridge University, Cambridge, U.K., in 1990.

He is an Associate Professor with the School of Electrical and Electronic Engineering. Nanyang Technological University (NTU), Singapore. He is also the Program Director for Mobile Robotics of the Center for Intelligent Machines, NTU. He was previously the Head of the Department of Computer Science and Engineering, University of Moratuwa. His research interests are in autonomous land and underwater vehicles, with an emphasis on problems related to navigation and perception.

Dr. Wijesoma is a member of the British Computer Society and a Chartered Information Systems Engineer (C. Eng.) of the Engineering Council of the U.K. He is a founding committee member of the IEEE Systems, Man, and Cybernetics Society Chapter, Singapore, Committee Member of IEEE Oceanic Engineering Society Chapter, Singapore. and Technical Co-chair of OCEANS'06 Asia Pacific IEEE Conference, Singapore.

L. D. L. Perera received the B.Sc. engineering (Hons) degree in electrical engineering from the University of Moratuwa, Moratuwa, Sri Lanka, in 1997. He is currently working toward the Ph.D. degree in mobile robotics at Nanyang Technological University, Singapore.

His research interests are in estimation theoretic mobile robot navigation algorithms, sensor fusion, multiple target tracking, and data association.

Martin D. Adams received the degree in engineering science and the D.Phil degree from the University of Oxford, Oxford, U.K., in 1988 and 1992, respectively.

He continued his research in autonomous robot navigation as a Project Leader and part-time Lecturer with the Institute of Robotics, Swiss Federal Institute of Technology (ETH), Zurich, Switzerland. He was a Guest Professor and taught control theory in St. Gallen, Switzerland, from 1994 to 1995. From 1996 to 2000, he served as a Senior Research Scientist of robotics and control, in the field of semiconductor assembly automation, with the European Semiconductor Equipment Centre (ESEC), Switzerland. He is currently an Associate Professor with the School of Electrical and Electronic Engineering, Nanyang Technological University (NTU), Singapore. He has published many articles in top ranking robotics journals and conferences, as well as various book chapters and a monograph. He has also been serving as an Associate Editor of a leading international journal. His research interests include sensor data processing for robot navigation, SLAM, inertial navigation, and sensor fusion. He has been a Principal Investigator for various robotics projects at NTU, and currently leads a collaborative research project providing autonomous cleaning agents within Singapore's largest theme park.